

Tuning the Bipolar Conductance of an Alkali-Doped C₆₀ Layer Sandwiched between Two Tunneling Barriers

Nilay A. Pradhan, Ning Liu, Christophe Silien,[†] and Wilson Ho*

Department of Physics and Astronomy and Department of Chemistry,
University of California, Irvine, California 92697-4575, USA

Received October 1, 2004; Revised Manuscript Received November 29, 2004

ABSTRACT

Resonant tunneling through a C₆₀ monolayer doped with single Na, K, Rb, and Cs atoms was measured between the tip of a scanning tunneling microscope and a NiAl(110) substrate. By supporting the monolayer on a thin aluminum oxide film grown on the substrate, a double barrier tunnel junction is formed, consisting of the vacuum and oxide. This geometry enables conductance through an electronic state of the alkali-C₆₀ complex at both positive and negative sample bias. The positions of the conductance peaks can be varied by tuning the vacuum barrier. An opposite variation is found for Na and K as compared to Rb and Cs, suggesting the influence of bonding on nanoscale transport.

Recent experiments on tunneling phenomena in nanostructures have provided an understanding of the role of impurities in electron transport.^{1,2} However, in most cases, it is difficult to ascertain the nature or the location of the impurities and thus to precisely determine the mechanism of their effects on the transport process. Needless to say, additional insight would be gained by adopting an approach that incorporates the resolution of the local electronic structure. It is also important to choose a system whose components are well characterized, so that greater emphasis can be placed on their mutual interactions and their imprint on experimentally measurable quantities.

Toward this end, the scanning tunneling microscope (STM) is unique in its ability to provide spatial and spectroscopic resolution at the atomic scale and has been widely used to reveal the electronic structure with submolecular precision.^{3–6} In this letter, we report the measurements of differential conductance spectra in the tunneling junction comprising an Ag tip, a vacuum barrier, an alkali-C₆₀ complex, an Al₂O₃ insulating layer, and a NiAl(110) substrate. Our results reveal the influence of the potential at the position of the complex on the transport properties. This junction geometry is adopted in order to create a double barrier tunneling junction and to isolate the alkali-C₆₀ system from either electrode.^{7–10} The extensive knowledge of the properties of the alkali-doped fullerenes and their relevance to superconductivity and electronic devices are also important factors behind the choice of this system.^{11,12}

The experiments were performed with a homemade variable temperature, ultrahigh vacuum STM based on a design detailed elsewhere.¹³ All the measurements were carried out at 11 K at a base pressure lower than 3×10^{-11} Torr. The differential conductance (dI/dV) was measured with lock-in detection of the ac tunneling current by modulating the sample bias (~ 10 mV, ~ 260 Hz) while keeping the feedback loop open. The Al₂O₃/NiAl(110) sample and Ag tip were prepared according to procedures described elsewhere.¹⁴ The C₆₀ (Aldrich, 99.9% purity) was sublimated from an alumina crucible onto the clean, partially oxidized sample at room temperature. The alkali atoms were evaporated in situ from commercial sources (SAES Getter) and deposited on C₆₀/Al₂O₃/NiAl(110) at 11 K.

C₆₀ forms a triangular structure with a lattice constant of 10 Å, which is close to the nearest neighbor distance in fullerite.¹² The molecules assume different orientations. In comparison to C₆₀ on NiAl(110) and other metals,^{6,15} the dI/dV spectra of C₆₀ on Al₂O₃/NiAl(110) are nearly independent of the tip location along the surface. The spectra exhibit a conductance gap stretching from -2.4 V to $+0.45$ V. The alkali atoms bond predominantly with the nearest neighbor C₆₀ and form well-defined complexes within the monolayer. The larger alkali atoms, K, Rb, and Cs appear as protrusions on the C₆₀ lattice, whereas Na is imaged as a depression¹⁶ (see insets in Figures 1 and 2).

In the case of Na, shown in Figure 1a, the dI/dV curve is initially recorded when the tunneling gap is set at 0.13 nA and 1.05 V. Subsequent spectra are measured after moving the tip either toward or away from the surface while keeping the feedback loop open.¹⁷ The weaker spectral features near

* Corresponding author: E-mail: wilsonho@uci.edu.

[†] On leave from Laboratoire de Spectroscopie Moléculaire de Surface, Facultés Universitaires Notre-Dame de la Paix, rue Bruxelles 61, B-5000 Namur, Belgium.

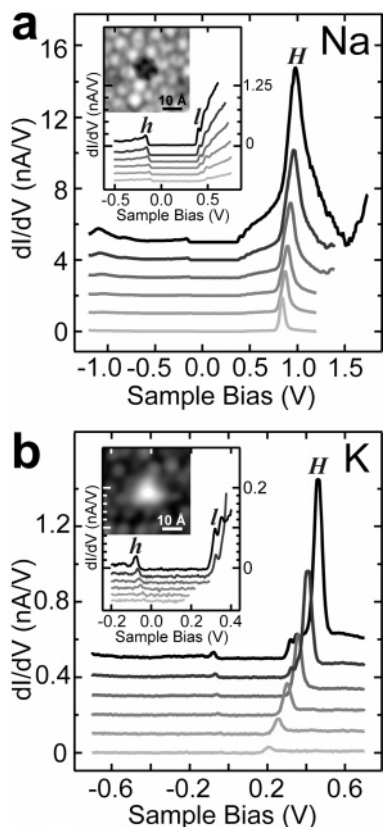


Figure 1. Differential conductance spectra as a function of tip–sample separation for individual alkali metal adatoms on $C_{60}/Al_2O_3/NiAl(110)$. (a) For Na, the tunneling gap is set initially at 0.13 nA and 1.05 V. Each curve is recorded by offsetting the tip by 0 Å (bottom curve) to -1.75 Å (top curve), decreasing the tip–sample separation in increments of 0.35 Å. Details of the curves near the Fermi level are shown in the inset. The spectra in the inset are scaled with respect to the corresponding spectra in the main figure by factors of (from top to bottom) 1, 1.5, 2, 2.5, 3, and 4. A topographic image of Na adatom on $C_{60}/Al_2O_3/NiAl(110)$ was recorded at 0.1 nA and 0.7 V. (b) Analogous spectra for the K atom, recorded with the tip–sample separation set initially at 30 pA and 0.7 V. The tip offsets are -0.35 Å (top curve) through $+1.4$ Å (bottom curve), in increments of 0.35 Å. A topographic image of K adatom measured at 15 pA and 1.5 V is also shown. The spectra in the inset have the same multiplication factors as those in the main figure. In (a) and (b), the HOMO (*h*, *H*) and LUMO (*l*, *L*) derived peaks are marked and described in the text. The sharp peaks and the corresponding lower intensity peaks are marked in capital and lower case letters, respectively. All the spectra are offset for clarity.

the Fermi level are magnified and shown in the inset. Figure 1b displays analogous data for K initially measured with the tunneling gap set at 30 pA and 0.7 V. Similarly, in Figure 2a and 2b we show the data for Rb and Cs, respectively, measured with the initial gap set at 0.1 nA and 1.5 V and 0.1 nA and 1.4 V, respectively. Intense, sharp conductance peaks are detected for all alkali metals. They are seen only at positive bias for Na and K for the range displayed^{18,19} (see peak *H* in Figure 1a and 1b), whereas they are observed at both bias polarities in the case of Rb and Cs (see peaks *H* and *L* in Figure 2a and 2b).

We associate the tall peak *H* at positive bias with the first peak *h* of a series of peaks at negative bias. This series of peaks is attributed to a progression of vibronic states within

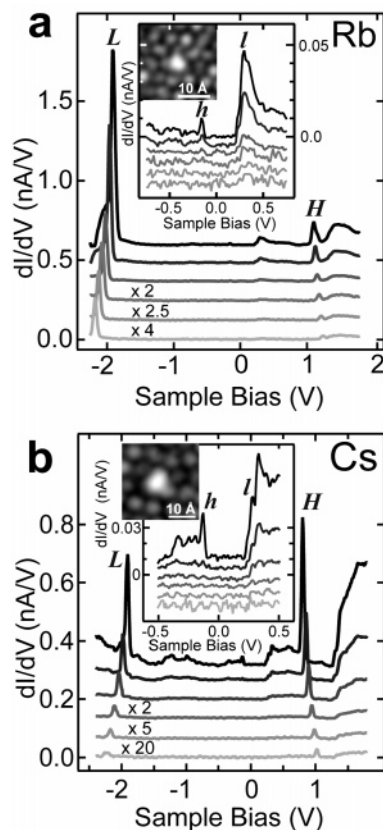


Figure 2. (a) dI/dV spectra, similar to Figure 1, for a Rb adatom with the initial tunneling gap set at 0.1 nA and 1.5 V, and offset in 0.35 Å increments from $+0.35$ Å (top curve) through $+2.1$ Å (bottom curve). Image of a Rb adatom observed at 0.1 nA and 1.4 V. (b) For a Cs adatom, the curves are measured with the initial gap set at 0.1 nA and 1.4 V and offsetting the tip in 0.35 Å increments from 0 Å (top curve) to $+1.75$ Å (bottom curve). The image of the Cs adatom was recorded at 0.1 nA and 1.5 V. The spectra in the inset bear the same multiplication factors as those in the main figures for both species of alkali atoms. The HOMO (*h*, *H*) and LUMO (*l*, *L*) derived peaks are marked as described in the text. All the spectra are offset for clarity.

the highest occupied molecular orbital (HOMO) of the complex.^{14,21} Similarly, the peak *L* at negative bias for Rb and Cs is associated with the first peak *l* of a series of peaks observed at positive bias corresponding to a progression of vibronic states within the lowest unoccupied molecular orbital (LUMO) of the alkali- C_{60} complex. The assignment of these spectral features is not initially obvious, attributing spectral features at both bias polarities to the same electronic state. We shall address this issue in the remainder of this letter, focusing on the resonances *h* and *H* since they are observed for all alkali metals.

In all cases, the *H* resonance shifts when the tip–sample distance (z) is changed. For Rb and Cs, the position of *H* shifts to larger bias values as z is increased, while in the case of Na and K, the opposite trend is seen. The positions of the peaks *h* and *H* are plotted in Figure 3a and 3b, respectively. For Na and K, the HOMO derived peak *h* of the vibronic progression shows a clear shift, whereas for Rb and Cs, the shift is much smaller. Similarly, shifts in *l* and *L* peaks are shown in Figure 3c and 3d. The origin of these shifts is schematically revealed in Figure 4.

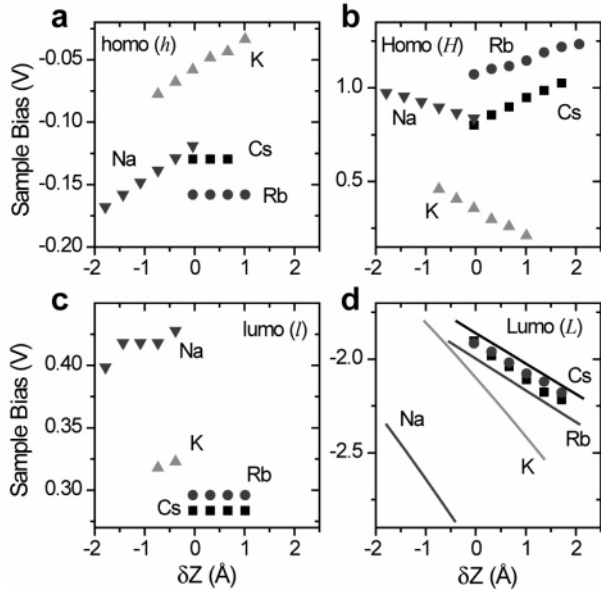


Figure 3. Summary of measured (symbols) and calculated (solid lines) values for the peaks shown in Figures 1 and 2. (a) Observed positions of the HOMO peak h for the alkali atoms Na, K, Rb, Cs as a function of the deviation from the initial tunneling gap settings. (b) Observed positions of the HOMO peak H . (c) Values of LUMO peak l measured for the alkali atoms. (d) Values of the LUMO peak L for Rb and Cs compared to the computed values obtained from the model described in the text using the data shown in (a), (b), and (c). Higher bias voltages are computed for Na and K where these adatoms are found to be unstable.

To explain the experimental results described above, we must examine the electric potential applied to the complex (V_a) and its dependence on z . We use a simplified model, that of a localized charge distribution lying between two barriers, vacuum and dielectric (consisting of the C_{60}/Al_2O_3 layer). The sample bias across the junction V_b (voltage between tip and NiAl) is thus divided between the vacuum and the dielectric barriers. Since the complex is in contact with the vacuum barrier at one end and with the oxide barrier at the other, we can use the simplified model if we now consider d/ϵ to be the effective thickness of the dielectric barrier; we have (see Figure 4),

$$V_a = \frac{d/\epsilon}{d/\epsilon + z} V_b \quad (1)$$

Let Δ be the magnitude of the HOMO energy relative to the Fermi level at zero bias. As shown in Figure 4a, the HOMO state contributes to the electronic transport when its position is raised above the Fermi level of the NiAl [$E_F(\text{NiAl})$] or the tip [$E_F(\text{tip})$] lowered below it. For a given z , the smallest magnitude of the negative bias required for the electrons to tunnel through the HOMO, V_b^h is $\Delta + V_a$, accounting for both the energy of the state (Δ) and the voltage drop across the dielectric (oxide) V_a , (see Figure 4a,i):

$$V_b^h = \left(1 + \frac{d}{\epsilon(z_0 + \delta z)}\right) \Delta \quad (2)$$

Here, z is written as the sum of the initial tip-complex

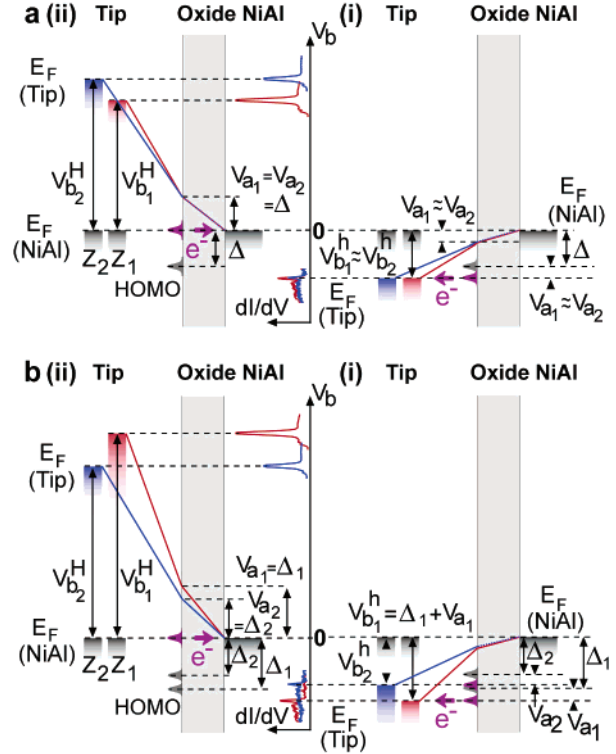


Figure 4. Schematic diagram of the tunneling process and the resultant peak movement consistent with the observations and eqs 1–5 in the text. (a) Proposed mechanism when the energy of the HOMO state Δ is constant and applicable to Rb and Cs. V_a represents the potential energy of the electron at the position of the complex (taken to be the voltage drop across the oxide) and $V_b^{h,H}$ denotes the bias values between the tip and the NiAl sample for which the peak is observed in the dI/dV spectrum for (i) negative and (ii) positive bias, respectively. The relationship between V_a and V_b for each bias polarity is described in the text. The subscripts 1 and 2 denote the position of the tip at distances z_1 and z_2 from the complex ($z_2 > z_1$), respectively. The direction of electron transport and the alignment of the alkali- C_{60} resonance with the appropriate Fermi level are indicated by the thick arrow. (b) Mechanism explaining the peak shift in the case of Na and K. Δ decreases ($\Delta_2 < \Delta_1$) when the tip is moved away from the complex ($z_1 < z_2$). This makes $V_{b_2}^h < V_{b_1}^h$, in contrast to that shown in a(ii). The dependence of Δ with z is described in the text. All the symbols have the same meaning as in (a).

separation z_0 and an experimentally controlled offset δz . Since Δ may, in principle vary when z is changed, we have

$$\frac{\partial V_b^h}{\partial z} = -\frac{d}{\epsilon(z_0 + \delta z)^2} \Delta + \left(1 + \frac{d}{\epsilon(z_0 + \delta z)}\right) \frac{\partial \Delta}{\partial z} \quad (3)$$

At positive bias, the electron can tunnel out of the HOMO state if its energy rises above the Fermi level of NiAl (see Figure 4a,ii). This condition is met when the sample bias is larger than

$$V_b^H = \left(1 + \frac{\epsilon(z_0 + \delta z)}{d}\right) \Delta \quad (4)$$

or

$$\frac{\partial V_b^H}{\partial z} = \frac{\epsilon\Delta}{d} + \left(1 + \frac{\epsilon(z_0 + \delta z)}{d}\right) \frac{\partial \Delta}{\partial z} \quad (5)$$

Given that the larger voltage drop is across the vacuum barrier, and if Δ does not depend on z , eqs 2 and 3 show that V_b^h is a slowly varying function of z (see Figure 4a,i). On the other hand eqs 4 and 5 indicate that V_b^H increases linearly with z (see Figure 4a,ii). Both of these trends are in agreement with the behavior of h and H for Rb and Cs (see Figure 3a,b). However, for Na and K, the approximation of a constant Δ is inconsistent with the experimental results. Since a clearly measurable shift is observed for $V_b^h(h)$ and $V_b^H(H)$ that decreases in magnitude with increasing z (Figure 3a, 3b), we are led to conclude that the value of $\partial\Delta/\partial z$ cannot be ignored in eqs 3 and 5 for Na and K. Similar analysis and set of equations apply to the LUMO (peaks I and L).

To verify the validity of the above model, we have computed the shift in the positions of the LUMO I , L peaks (see Figure 3c,d) using eqs 2 and 4 and the experimentally determined quantities V_b^h , V_b^H , and δz . Numerical fitting of the ratio of eqs 2 and 4 and their LUMO analogues to 17 datasets of the z -evolution for pairs of peaks [either (h, H) or (I, L)] yields $d/\epsilon = 1.5 \pm 0.4 \text{ \AA}$. This value is then used to calculate the initial tip-complex distance z_0 for each dataset, by substituting the HOMO data (h and H peak positions) into the same equations. The variations in $z_0 \approx 10 \text{ \AA}$ are due to different initial tunneling conditions. The Δ of the LUMO is obtained using the expression for V_b^I (analogous to eq 2). Knowing Δ , d/ϵ and z_0 , the positions of the L peaks are deduced by substitution into V_b^L (analogous to eq 4). As seen from Figure 3d, a close agreement is reached for both Rb and Cs. The slight discrepancies between the calculated and observed values can be traced to the simplicity of the model, where, for example, the voltage drop across the complex is neglected. Since no data on the L peaks are available for Na and K, our calculations simply indicate the expected trend of peak L in these cases.

As seen above, the energy position of the vibronic state Δ and its dependence on z is critical in understanding the anomalous shift of the sharp peak for Na and K. Upon adsorption on the fullerene layer, alkali atoms are known to transfer almost one electron to the neighboring molecules,¹² leading to the formation of the alkali-C₆₀ complexes. It is possible that the alkali atoms are intercalated in the C₆₀ monolayer during the formation of the complex,^{22,23} but this cannot be definitively inferred from our STM images alone. Although we do not know the exact charge distribution within the complex, it is expected to have a dipolar component.²⁴ The energy level of the complex (Δ) depends on the image potential of the charge distribution in the NiAl substrate as well as in the Ag tip and consequently on the distance between the tip and the complex (z). The contribution from the image dipoles in the tip at the complex is proportional to $O(-p^2/z^3)$, where p is the magnitude of the dipole moment. Consequently, this contribution tends to lower the HOMO level of the complex as the tip gets closer to the sample. This contribution to the state energy opposes the one due to the reduced voltage drop across the vacuum

as the tip is brought closer, especially if the magnitude of the dipole moment is appreciable. This makes $\partial\Delta/\partial z$ negative and gives the correct trend for Na and K. On the other hand, the negligible changes in the values of V_b^h in Figure 2 correctly explain the trend for Rb and Cs (also see Figure 3d). Using this argument the data suggest a much smaller value of $\partial\Delta/\partial z$ for Rb and Cs. However, at present, a satisfactory explanation of the physical origin of these effects is unclear. Detailed electronic structure calculations, complementing the experimental results, are needed in order to fully understand the bonding of the alkali atoms on C₆₀/Al₂O₃/NiAl(110). However, these calculations are beyond the scope of the present study.

This letter demonstrates the possibility that a single electronic state (HOMO or LUMO) contributes to the conductance at both polarities of bias. This observation is enabled by designing and fabricating a double-barrier junction, defined by a Ag tip, a vacuum barrier, an alkali-C₆₀ complex, an Al₂O₃ insulating layer, and a NiAl(110) substrate. In addition, depending on the alkali species, the differential conductance exhibits anomalous behavior that depends on the voltage distribution in the junction and variation of the electronic state energy with the thickness of the vacuum barrier. The precision and control provided by the STM reveal factors influencing charge transport that are not easily characterizable in other experimental geometries. These results provide a new understanding about the effects of single impurity doping, which is of prime interest in the nanoscale fabrication of electronic devices on oxide and other insulators.

Acknowledgment. This material is based on work supported by the Air Force Office of Scientific Research (Grant No. FA9550-04-1-0181). The authors are grateful to X. Chen, G. V. Nazin, X. H. Qiu, and S. W. Wu for many insights and inspiring discussions. C.S. is a scientific research scholar of the Belgian National Fund for Scientific Research (FNRS).

References

- (1) Lind, E.; Gustafson, B.; Pietzonka, I.; Wernersson, L.-E. *Phys. Rev. B* **2003**, *68*, 033312, and references therein.
- (2) Gryglas, M.; Baj, M.; Chenaud, B.; Jouault, B.; Cavanna, A.; Faini, G. *Phys. Rev. B* **2004**, *69*, 165302.
- (3) Hashizume, T.; Motai, K.; Wang, X.-D.; Shinohara, H.; Saito, Y.; Maruyama, Y.; Ohno, K.; Kawazoe, Y.; Nishina, Y.; Pickering, H. W.; Kuk, Y.; Sakurai, T. *Phys. Rev. Lett.* **1993**, *71*, 2959.
- (4) Grobis, M.; Lu, X.; Crommie, M. F. *Phys. Rev. B* **2002**, *66*, 161408.
- (5) Lu, X.; Grobis, M.; Khoo, K. H.; Louie, S. G.; Crommie, M. F. *Phys. Rev. Lett.* **2003**, *90*, 096802.
- (6) Silien, C.; Pradhan, N. A.; Ho, W.; Thiry, P. A. *Phys. Rev. B* **2004**, *69*, 115434.
- (7) Porath, D.; Levi, Y.; Tarabiah, M.; Millo, O. *Phys. Rev. B* **1997**, *56*, 9829.
- (8) Park, H.; Park, J.; Lim, A. K. L.; Anderson, E. H.; Alivisatos, A. P.; McEuen, P. L. *Nature* **2000**, *407*, 57.
- (9) Park, J.; Pasupathy, A. N.; Goldsmith, J. I.; Chang, C.; Yaish, Y.; Petta, J. R.; Rinkoski, M.; Sethna, J. P.; Abruña, H. D.; McEuen, P. L.; Ralph, D. C. *Nature* **2002**, *417*, 722.
- (10) Liang, W. J.; Shores, M. P.; Bockrath, M.; Long, J. R.; Park, H. *Nature* **2002**, *417*, 725.
- (11) Gunnarsson, O. *Rev. Mod. Phys.* **1997**, *69*, 575, and references therein.
- (12) Dresselhaus, M. S.; Dresselhaus, G.; Eklund, P. C. *Science of Fullerenes and Carbon Nanotubes*; Academic Press: San Diego, 1996.

- (13) Stipe, B. C.; Rezaei, M. A.; Ho, W. *Rev. Sci. Instrum.* **1999**, *70*, 137.
- (14) Liu, N.; Pradhan, N. A.; Ho, W. *J. Chem. Phys.* **2004**, *120*, 11371.
- (15) Rogero, C.; Pascual, J. I.; Gomez-Herrero, J.; Baro, A. M. *J. Chem. Phys.* **2002**, *116*, 832.
- (16) The topographic images convey the integrated local density of states (LDOS) measured at the tip apex in the vicinity of the alkali atom adsorption site and may not reflect the actual geometric structures on the surface. For example, in the case of Na, the depression in the image implies that the integrated LDOS over the atom is lower than the surrounding. It is also possible that due to its small size, the atom is located below the plane of the C₆₀ layer. However, it is unlikely that the Na atom penetrates the fullerene cage under the present experimental conditions. In an observation consistent with those reported here, we found that Li atoms, which are smaller than Na, are also imaged as depressions. See text and ref 23 for more details.
- (17) The changes in the distance between the tip and the surface, δz , can be determined to great accuracy in contrast to the absolute value for the distance z . This is because the complex nature of the substrate [C₆₀/Al₂O₃/NiAl(110)] makes it difficult to obtain the tip-sample distance by bringing the tip into contact with the substrate. In contrast, the incremental changes in tip-substrate distance can be experimentally controlled with great precision. Furthermore, we use δz since it is the shift in the peak position as a function of δz or the slope in the plot of the peak position versus δz that is important in the data analysis.
- (18) The complexes were found to be unstable beyond the voltage range displayed, irrespective of the tip height. When the tip is brought too close to the alkali-C₆₀ complex, or the bias exceeds a certain value depending on the alkali species, the atom desorbs, jumps away, or attaches onto the tip.
- (19) According to the model described in eqs 1–5 (see main text), the positions of the short (*h*, *I*) and the tall (*H*, *L*) peaks are related. Thus, the closer a short peak is to the Fermi level, the nearer is the corresponding sharp peak to zero bias, and vice versa. As can be seen from the insets in Figure 1, peaks *h* are much closer to E_F than their positive counterparts (*I*). This implies that to find the peak *L* corresponding to *I*, we have to increase the bias in the negative direction. Since Na-C₆₀ and K-C₆₀ complexes are unstable beyond the range shown in Figure 1, the bias at which peaks *L* occur cannot be attained. This lack of observation of *L*, however, does not contradict, but supports the proposed model.
- (20) The alkali atoms are thought to be in a cationic state since charge transfer is expected between the atom and the nearest neighbor C₆₀ molecules. These atoms adsorb as single atoms but are not isolated since they are adsorbed on a substrate. Individual atoms are also observed over the oxide film. However, they are unstable (except for Cs), and do not display any of the characteristics described in this paper, which are associated with the delocalized two-dimensional electronic state of the C₆₀ monolayer on Al₂O₃ thin film.
- (21) Qiu, X. H.; Nazin, G. V.; Ho, W. *Phys. Rev. Lett.* **2004**, *92*, 206102.
- (22) Silien, C.; Thiry, P. A.; Caudano, Y. *Surf. Sci.* **2004**, *174*, 558.
- (23) The smallest cavity radius for three C₆₀ molecules, R , is given by $R = a/\sqrt{3} - r$ where a and r are the C₆₀ lattice constant and radius, respectively. The radius of the cavity thus obtained using the values of a and r given in ref 12 is 2.22 Å. The covalent radii of Na, K, Rb, and Cs are 1.54, 1.96, 2.11, and 2.25 Å, respectively. The corresponding ionic radii are 1.02, 1.38, 1.52, and 1.67 Å (see ref 12).
- (24) Strictly speaking, the multipole expansion is valid only when the scale of the charge distribution is much smaller than the length scale of the measurement. Since this does not apply in our case, the full charge distribution must be considered for any meaningful predictions. This would require geometric details that cannot be inferred directly from the experiments. However, we anticipate that the electric potential due to the complex will have a dipolar term in the asymptotic limit (due to charge transfer between the alkali atoms and the fullerene molecules).

NL0483744